Chapter 12
Mapping a Profile Wall of a Typic Udipsamments from the Central Sands in Wisconsin, USA

Kabindra Adhikari, Alfred E. Hartemink and Budiman Minasny

Abstract We measured and mapped the spatial distribution of Al, Si, Fe, Mn, Ca, pH, soil moisture content (θ), and color of a soil profile wall of a Typic Udipsamments. A 10 × 10 cm grid was laid on the soil profile wall, and 70 soil samples were collected from the grid centers. The spatial distribution of these properties was mapped with block kriging. The kriged values of the elements and red color were used in *k*-means clustering to identify soil horizons. Variation in the profile was considerable, but we observed that Fe, Mn, Ca, pH, and θ decreased with soil depth, while red color increased. The concentration of Al and Si increased at depth between 30 and 60 cm from the soil surface. The *k*-means clustering was able to locate three soil horizons in the profile, which was comparable to the standard soil profile description. We found that pXRF and soil color index coupled with clustering could be useful in digital soil morphometrics for the identification of soil horizons.

Keywords Digital soil morphometrics · Soil horizons · pXRF · *k*-means clustering

12.1 Introduction

Soil profiles comprise of a number of layers or horizons, which are often parallel to the land surface and are less heterogeneous in terms of properties and processes by which they are formed. The horizons are more or less continuous one to another in geographic, temporal, and character space (FitzPatrick 1988). Generally, soil horizons are

K. Adhikari (✉) · A.E. Hartemink
Department of Soil Science, FD Hole Soils Lab, University of Wisconsin-Madison, Madison, WI 53706, USA
e-mail: kabindra.adhikari@wisc.edu

B. Minasny
Department of Environmental Sciences, The University of Sydney, Biomedical Building C81, Sydney, NSW 2006, Australia

formed by the addition or removal of materials and its translocation or transformation within the profile. In most profiles, horizons are distinct in color with sharp boundaries making it straightforward to differentiate, but in many soils, the color or other diagnostic property changes gradually so that the boundaries are difficult to establish (Brady and Weil 1996). Delineation of horizons in a soil profile needs a careful examination of soil properties, understanding of the physicochemical and biologic processes involved, and information on soil–landscape relations of the area where the profile is located. Bridges (1993) stated that it is impossible to ignore soil horizon designations, as they have become an integral part in soil science communications from local, national, and international levels.

In pedology, where describing soil profiles and horizons is important (Bockheim et al. 2005; Butler 1980; Kellogg 1974), a number of tools and techniques have been developed to observe and measure soil properties in situ or in the laboratory. The application of such tools and techniques for measuring and mapping soil properties, such as texture, structure, color, carbonates, moisture, mottles and redoximorphic features, pores and roots, and horizon depth and boundaries, is called digital soil morphometrics (Hartemink and Minasny 2014). Digital morphometrics employs tools such as electrical resistivity, ground-penetrating radar, portable X-ray florescence spectrometry (pXRF), Vis–NIR, digital cameras, and profile cone penetrometer to measure soil properties and in the identification and mapping of soil horizon depths and boundaries (e.g., Chaplot et al. 2001; Doolittle and Collins 1995; Fajardo et al. 2015; Rooney and Lowery 2000; Steffens and Buddenbaum 2013; Tabbagh et al. 2000; Weindorf et al. 2012). Among all, pXRF offers a way of quantifying elemental concentration in the soils and has been used for soil horizon identification (Weindorf et al. 2012). Similarly, usefulness of Vis–NIR coupled with fuzzy clustering has been reported to recognize soil morphological horizons from Australia (Fajardo et al. 2015). As the soil varies continuously with depth, modeling and mapping soil depth functions is important in digital soil morphometrics. Minasny et al. (2016) provide some insights into the distribution of soil properties as a function of depth, and Adhikari et al. (2013, 2014) report some examples of modeling and mapping soil properties' depth functions.

Soil profile data collected with different morphometric tools and its grouping or clustering based on similarities could be used to identify soil horizon boundaries. The use of k-means clustering has been used in soil horizon classification (McBratney and Gruijter 1992; Triantafilis et al. 2001). Data clustering is mostly done for grouping soil class on a lateral spatial extent. For example, Webster (1973) determined soil boundaries along transects automatically by calculating the Mahalanobis distance of the soil properties along a width "window." We use this principle for identifying horizon boundaries based on vertical measurements of a profile wall. This study aims to map the soil profile wall of a Typic Udipsamments using digital soil morphometrics. The objectives were (i) to map the spatial distribution of Al, Si, Fe, Mn, Ca, pH, θ, and soil color in the soil profile wall of 100 cm × 70 cm dimension and (ii) to use elemental concentration and soil color to identify soil horizons.

12.2   Materials and Methods

12.2.1   Study Site Description

The study site was located in Adams County in the central-south part of Wisconsin, USA (latitude 43° 53′ 41.82″N; longitude 89° 41′ 30.66″W). The area is known as Central Sands where soils are developed on glacial outwash and are relatively young (<15,000–17,000-year-old). Soils of this area were Plainfield series and classified as Mixed, mesic Typic Udipsamments (USDA 1999). A typical soil profile of a Plainfield series consists of four to five soil horizons: Ap ($\sim$0–18 cm), Bw1 ($\sim$18–41 cm), Bw2 ($\sim$41–71 cm), BC ($\sim$71–92 cm), and C (>92 cm). We have found that these soils under intensive agriculture have a topsoil depth of 29 cm. Topography in the study area is flat (1 % slope) with an elevation of about 325 m asl. These soils are under agriculture with sweet corn, potatoes, and soybean as main crops. The soils are irrigated with 200–300 mm of water annually. Figure 12.1 displays the location of the study site in the Central Sands with the distribution of entisols, including Udipsamments, in Wisconsin.

12.2.2   Soil Sampling

A soil profile of 1 m^3 dimension was opened in July. A 10 × 10 cm grid net was laid down on the profile wall covering 0.7 m^2 area, and the grid corners were marked with pegs (Fig. 12.1). Soils were sampled from each grid center and in total 70 samples were collected from the profile. Colors were determined with the Munsell color chart, and volumetric soil moisture content (θ) was measured with a time-domain reflectometry (TDR) (Spectrum FieldScout TDR 300). Each sample was air-dried, ground, and scanned in the laboratory with a Delta Professional pXRF Analyzer (Olympus Scientific Solutions Americas, Inc.) for 30 s in geochemical mode, and the data on elemental concentration of aluminum (Al), silica (Si), iron (Fe), manganese (Mn), and calcium (Ca) were collected. For the color, hue, value, and chroma obtained from the Munsell color chart were converted to red, green, and blue color coordinate using the algorithm for quantitative pedology package (Beaudette et al. 2013). Samples were analyzed for soil pH measured in water at a soil-to-water ratio of 1:1.

12.2.3   General Statistics and Mapping

The distribution of soil properties by depth was analyzed considering mean, standard deviation, median, CV, and interquartile range. Box plots of each soil property at each 10-cm soil depth interval were generated (SAS Institute Inc. 2013).
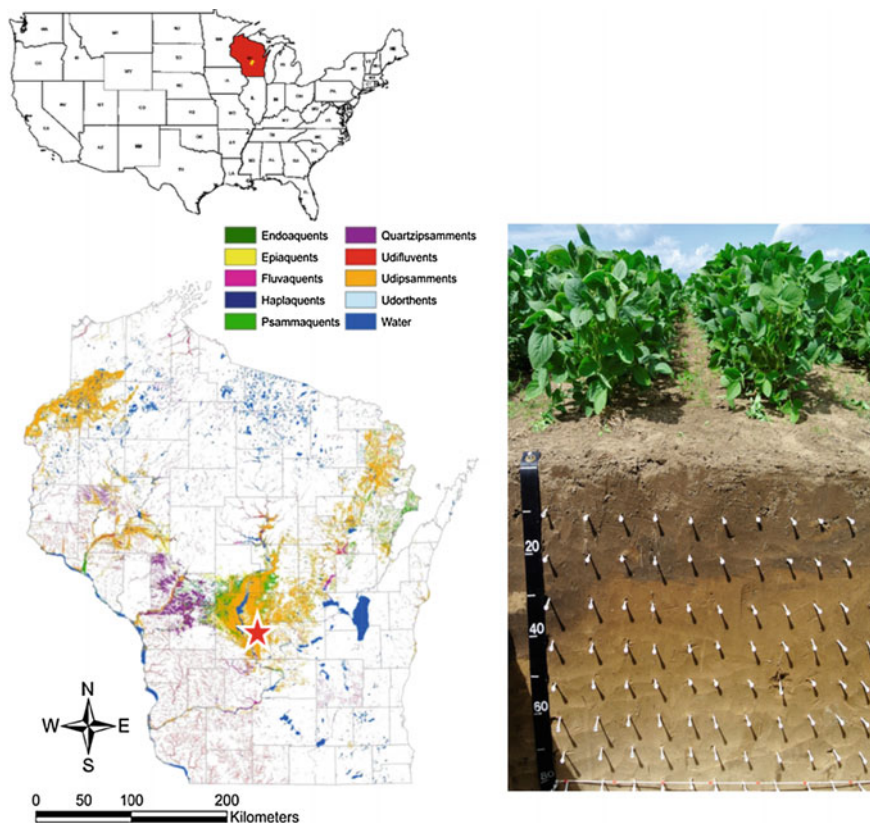
Fig. 12.1 Distribution of Udipsamments and the location of soil profile in Wisconsin. The profile wall displays the 10 × 10 cm grid net established for soil sampling

Autocorrelation and spatial distribution of the selected soil properties on the profile wall were analyzed and mapped using isotropic variogram and block kriging using Vesper (Minasny et al. 2005). We used block kriging of 10 cm × 10 cm size over the point kriging because we assumed it represents the average value of the property for that grid. Spatial dependency of the soil properties was evaluated with nugget-to-sill ratio (*NSR*) with *NSR* < 0.25, strong; 0.25 < *NSR* > 0.75, moderate; and *NSR* > 0.75, weak spatial dependence (Cambardella et al. 1994).

$$NSR = \frac{C_0}{C_0 + C_1} \qquad (12.1)$$

where C_0 and C_1 are the nugget and partial sill of the variogram model.

12.2.4   k-*Means Clustering*

We grouped the values of the measured soil properties based on similarities using *k*-means clustering algorithm (MacQueen 1967). The *k*-means is a common unsupervised learning algorithm to classify a given data set through a certain number of clusters fixed a priori. The objective function of the *k*-means aims at minimizing the squared error function (Eq. 12.2):

$$J = \sum_{j=1}^{k} \sum_{i=1}^{k} \left\| x_i^{(j)} - c_j \right\|^2 \tag{12.2}$$

where $\left\| x_i^{(j)} - c_j \right\|^2$ is a chosen distance measured between data point $x_i^{(j)}$ and the cluster center c_j and indicates the distance of the *n* data points from their respective cluster centers.

The clustering analysis was done in JMP software (SAS Institute Inc. 2013) using the block-kriged values of Al, Si, Fe, Mn, Ca, and red color as inputs. The procedure was as follows:

1. Define the number of clusters or seeds (*k*-cluster);
2. Assign each observation to the closest cluster;
3. Calculate the centroid of each cluster (*k* centroid);
4. Replace seeds with centroid and reassign the observations; and
5. Continue until the clusters are stable.

We clustered the soil properties' values with the initial cluster set to two and then repeated the process with subsequently increasing the cluster numbers to five assuming two to five soil horizons within 70 cm depth.

12.2.5   *Selecting the Cluster*

Once the values were partitioned into four different cluster sets (*k* = 2, 3, 4, 5), they were displayed as corresponding cluster maps. Among the four different cluster maps, the best map that represents the observed soil horizon boundaries was selected using the cubic clustering criterion (*CCC*). The *CCC* can be used to estimate the optimum number of clusters in *k*-means clustering. It compares the R^2 of clusters with the R^2 of a uniformly distributed set of points with the highest *CCC* value for the most optimal cluster set. The *CCC* can be computed from the observed R^2.

$$CCC = \ln\left[\frac{1 - E(R^2)}{1 - R^2}\right] \frac{\sqrt{\frac{np^*}{2}}}{(0.001 + E(R^2))^{1.2}} \tag{12.3}$$

where $E(R^2)$ the expected value of R^2 derived from extensive simulations, n the number of observations, and p^* the between cluster variation.

12.3   Results

12.3.1   Soil Properties

Descriptive statistics of soil properties from the soil profile wall are given in Table 12.1. Among the soil properties, Mn was most highly variable (CV = 48 %) followed by Al and Si (CV = 33 and 32 %, respectively), whereas the pH was least variable (CV = 5 %). Average Fe content of the profile was 5197 mg kg^{-1} with a CV of 32 % which is comparable to Si (CV = 32 %) but was slightly higher than that of Ca (CV = 26 %). With soil depth, the average value of Al and Si increased to 50/60 cm below the surface and decreased thereafter. The Fe levels decreased with soil depth, but the decrease was gradual with the lowest Fe levels at 60–70 cm depth. The levels of Mn and Ca were high in the surface layer and decreased with depth. The maximum variation of Fe and Ca was observed at 0–10 cm depth. Similarly, pH and soil moisture were higher and less variable in the surface layers, but variation increased below 30 cm. The red color was at lowest and more variable in the surface and increased sharply with depth, with maximum values at 60–70 cm soil depth. The variation of Al and Si was maximum at 20–30 cm soil depth and minimum at 30–40 cm. Figure 12.2 shows the box plots of the soil properties at 0–70 cm depth.

12.3.2   Maps of Soil Properties

The variogram parameters used for each soil property mapping are listed in Table 12.2. The levels of Ca showed a short limited variation compared to other

Table 12.1 Descriptive statistics of measured soil properties from the profile wall (dimension 100 cm × 70 cm)

Soil property	Aluminum (mg/kg)	Silica (mg/kg)	Iron (mg/kg)	Manganese (mg/kg)	Calcium (mg/kg)	Red color index	pH	Moisture (cm³/cm³)
Minimum	3000	15,018	1955	0	2522	111	5.3	6.2
Maximum	11,800	104,300	10,890	479	8480	201	6.5	18.1
Mean	7267	73,726	5197	121	3947	152	5.9	12.1
(± SD)	(±2451)	(±23,518)	(±1608)	(±107)	(±1033)	(±26)	(±0.3)	(±2.5)
CV, %	33.7	31.9	30.9	48.7	26.2	17.1	5.3	21.1
Median	7600	81,950	5715	98	3619	148	5.8	12.5
IQ range	4275	23,049	1893	213	1114	33	0.5	4.1
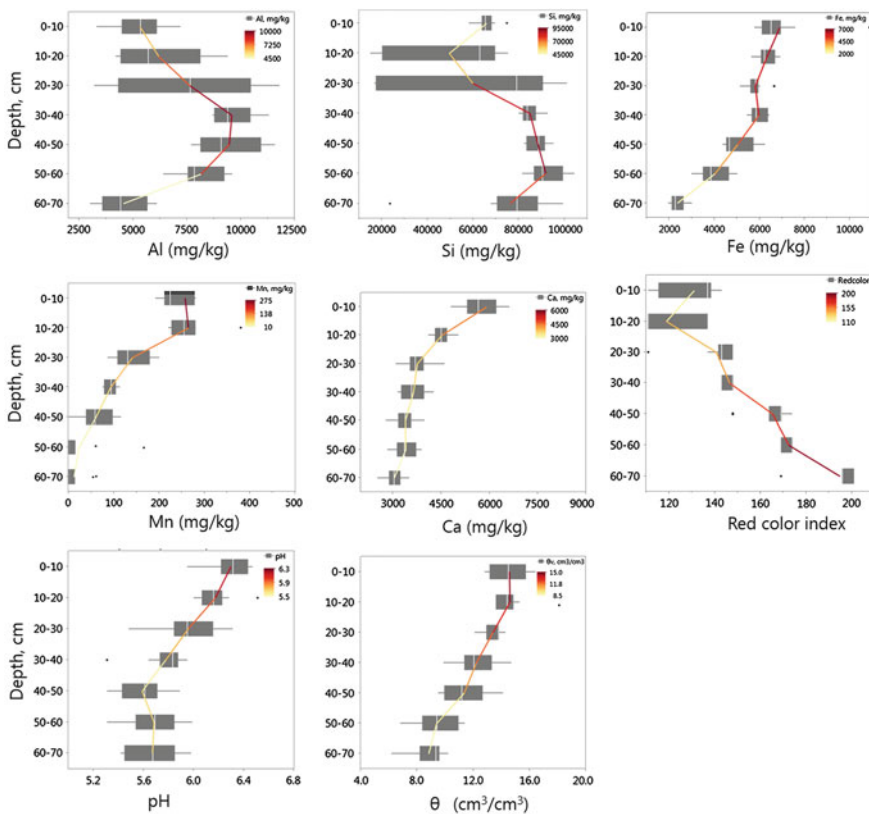
Fig. 12.2 Box plots showing the depthwise distribution of aluminum (Al), silica (Si), iron (Fe), manganese (Mn), calcium (Ca), red color index, pH, and soil moisture (θ) at each 10 cm depth increment in the soil profile. The continuous line represents the average value of measured soil properties and the values increases from yellow to dark red

Table 12.2 Variogram parameters of soil properties

Soil property	Variogram model	C_0^a (mg/kg)^2	C_1^a (mg/kg)^2	A, cm	NSR^a
Aluminum	Exponential	851,364	6,002,548	37	0.12
Silica	Spherical	209×10^5	377×10^5	39	0.26
Iron	Gaussian	208,183	3,249,967	38	0.06
Manganese	Gaussian	1689	15,787	42	0.10
Calcium	Gaussian	2262	10,000	33	0.18
Red color index	Gaussian	80	1006	45	0.07
pH	Spherical	0.01	0.12	50	0.08
Soil moisture	Gaussian	0.62	8.6	35	0.07

[a]C_0 nugget; C_1 partial sill; A range; and NSR nugget-to-sill ratio

elements, all sharing a comparable range between 33 and 42 cm, but pH had the highest range of 60 cm and was least variable (CV = 5.3 %). All soil properties had strong spatial dependence (NSR < 0.25) except for Si which showed a moderate spatial dependence (NSR = 0.36). The predicted maps (Fig. 12.3) of Ca, Mn, and Fe showed that these elements were mostly confined to the surface horizons with Ca mostly within the top 20 cm, Mn to 40 cm, and Fe to 50 cm depth. The red color increased with depth where maximum values were recorded below 60 cm. The concentration of Si, and Al, was higher at 25–60 cm, and a lower level of Al was also recorded below 60 cm. Soil pH was higher at 0–20 cm and decreased below 30 cm. The pH map was irregular and patchy. Soil moisture showed a similar pattern with higher values at the surface. The soil moisture map also reflected the crop row (soybean) influence with relatively lower moisture content between the crop rows.

12.3.3 Cluster Maps and Soil Horizons

Clustering of the kriged values of soil properties produced four maps (Fig. 12.4), each for one set of a defined cluster (k = 2, 3, 4, and 5). For cluster two and three, the first horizon boundary is at a depth of about 30 cm (Fig. 12.4a, b) and the second horizon boundary at about 55 cm depth (Fig. 12.4b). Cluster four divides each of the first and second horizons of cluster two (Fig. 12.4a) into two new horizons (Fig. 12.4c). Cluster five defined a small portion of the first horizon as a possible new horizon (Fig. 12.4d). For all cluster maps except cluster two, the last horizon boundary is at a same depth of about 55–60 cm from the soil surface.

   Among the four cluster maps, the highest CCC was found for cluster three (CCC = 49.6) (Fig. 12.5a). Cluster two had the lowest CCC of about 15 and that for cluster five was 46. Cluster three was selected to represent soil horizon boundaries in the profile. Figure 12.5b plots the points and clusters in the first two principle components of the input data (i.e., PC1 and PC2) that exceeded the eigenvalue of 1. The eigenvalues for PC1 and PC2 were 4.2 and 1.4, respectively. Soil properties falling along PC1 axis were Ca, Mn, and red color index, whereas those along PC2 were Al and Si with higher loadings of these elements. Fe content, however, was between the two PCs with a moderate loading.

   For the selected cluster, Table 12.3 lists the mean and standard deviation of the soil properties in each cluster. For cluster one, Mn was the most variable element (CV = 75 %) followed by Fe (CV = 25 %). Ca and red color index both shared a similar variability (CV = 4.3 %). Cluster one had the maximum average for red color index, whereas cluster two had the lowest Si but highest Fe, Mn, and Ca. A maximum level of Si and Al was present in cluster three.

   A positive correlation was found between the elements Al and Si, and Fe with Mn and Ca. Red color index had a negative correlation with Mn, and Ca, and a positive correlation with Si. Similarly, both Al and Si were negatively correlated with Ca and Mn. The Al levels showed no relation with Fe, with the red color index (Fig. 12.6).
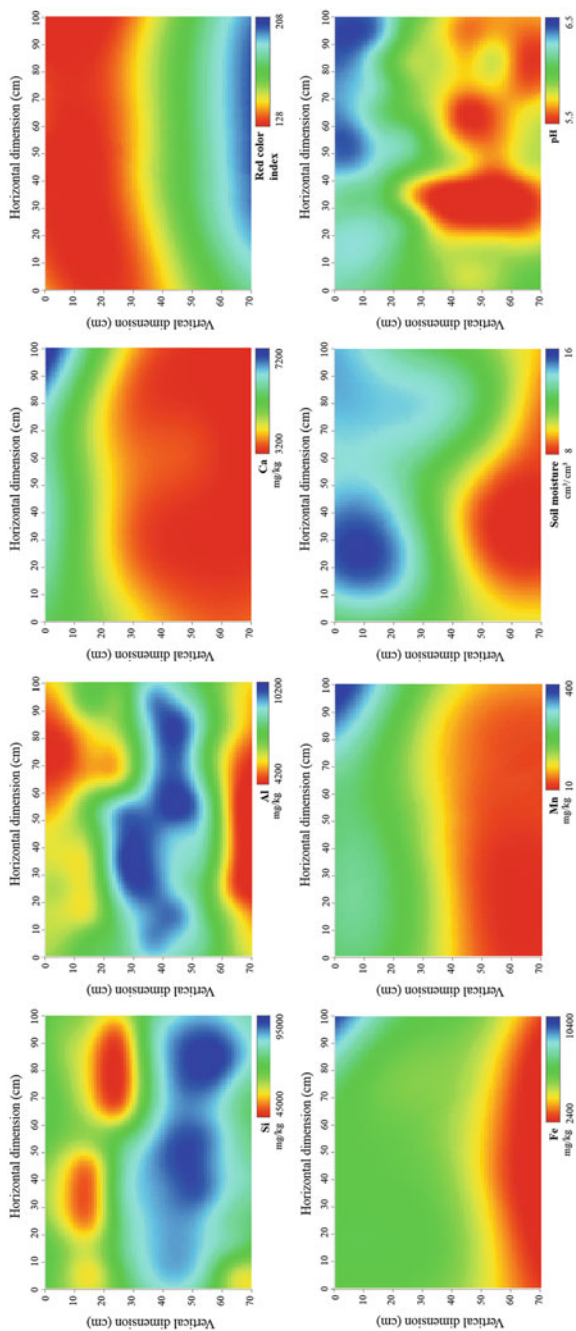
Fig. 12.3 Kriged maps showing the spatial distribution of measured soil properties in the soil profile (dimension 100 cm × 70 cm)
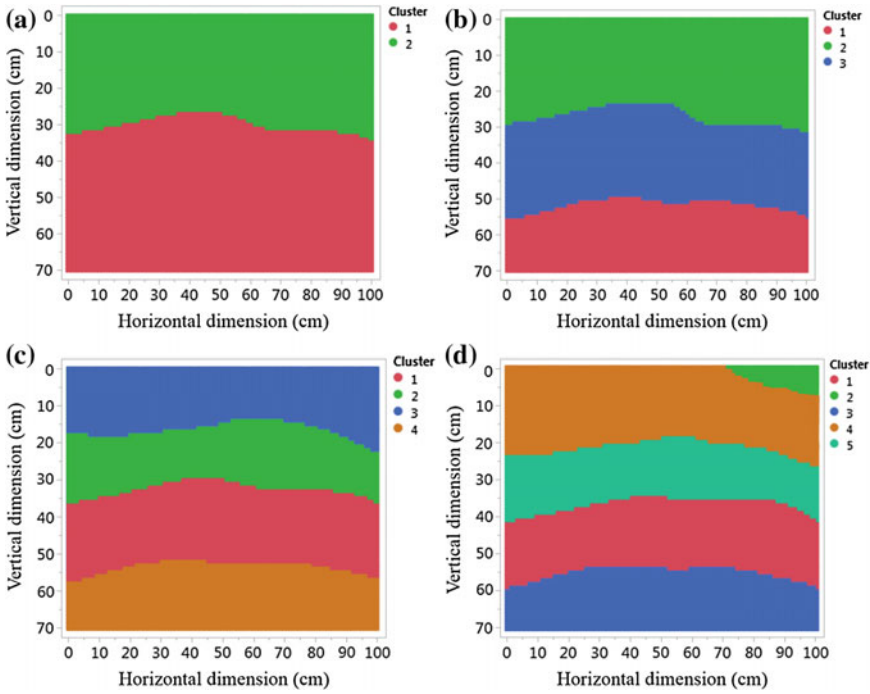
Fig. 12.4 Map of four different sets of *k*-clusters; **a** *k* = 2; **b** *k* = 3; **c** *k* = 4; and **d** *k* = 5, showing possible horizon boundaries in the profile wall
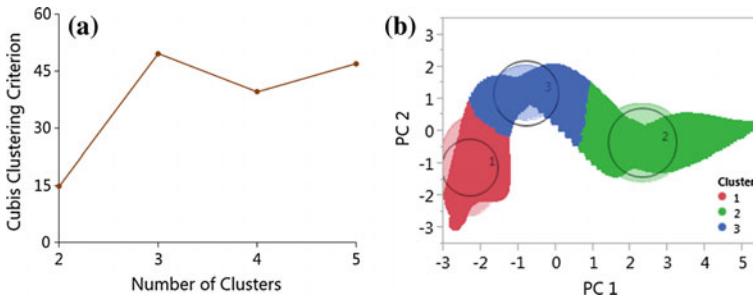
Fig. 12.5 **a** Plot of cubic clustering criterion versus number of *k*-cluster sets and **b** the first two principle components (PCs) of the points (*dark color*) and of the most appropriate cluster set (*k* = 3) indicated as *light color*

Based on the observations, the soil profile had three horizons, namely Ap (∼0–18 cm), Bw1 (∼18–41 cm), and Bw2 (∼41–71 cm). The cluster map suggested the three horizons, but the depth of these horizon boundaries was deeper than that of the observed horizon depth. We found that the depth of Ap horizon ranged between 0 and 27/30 cm, Bw1 between 27 and 30/54 cm, and Bw2 from 54 to >70 cm (Fig. 12.4b).

Table 12.3 Mean and standard deviation of soil properties for the selected cluster set ($k = 3$)

Cluster	Aluminum		Silica		Iron		Manganese		Calcium		Red color index	
	Avg.[a] (mg/kg)	Stdev.[a] (mg/kg)	Avg. (mg/kg)	Stdev. (mg/kg)	Avg. (mg/kg)	Stdev. (mg/kg)	Avg. (mg/kg)	Stdev. (mg/kg)	Avg. (mg/kg)	Stdev. (mg/kg)	Avg. (mg/kg)	Stdev. (mg/kg)
1	6230.9	1363.1	82,142.2	7513.6	3057.5	771.7	19.5	14.8	3223.2	139.9	186.0	8.1
2	6212.1	1062.1	59,937.1	6837.4	6449.4	647.3	227.1	47.8	4892.5	735.2	129.6	4.0
3	9094.7	630.5	82,654.0	7276.3	5389.7	557.2	82.1	40.1	3505.7	194.3	154.1	11.3

[a]*Avg.* mean value; *Stdev.* standard deviation
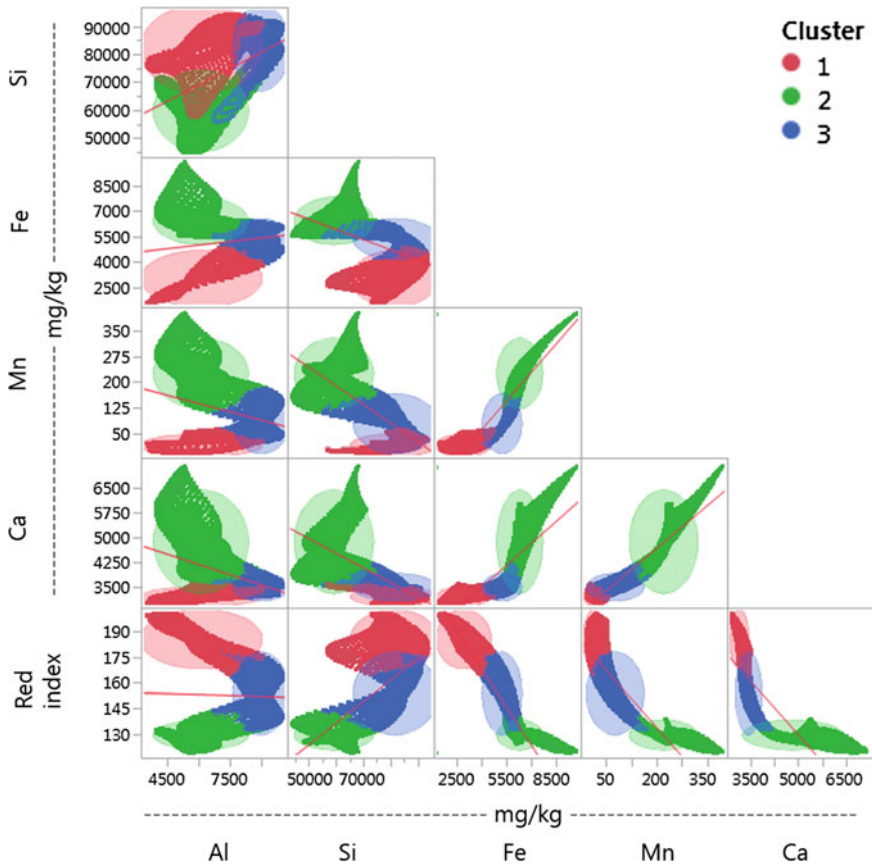
Fig. 12.6 Scatterplot matrix of soil attributes for the most appropriate cluster ($k = 3$). *Light color* represents the cluster of the points in *darker color*

12.4 Discussion

12.4.1 Digital Soil Morphometrics

This study applied digital soil morphometric tools and techniques to collect soil data and identify soil horizon boundaries of an Udipsamments profile wall. A grid-based soil sampling design ensured capturing the variations of soil properties across the profile wall. Data collection using pXRF and TDR helped to understand soil properties' variations in a profile wall both in horizontal and in vertical dimensions. The use of pXRF in soil properties' data collection and evaluation has been reported in other studies (e.g., Grauer-Gray and Hartemink 2016; Stockmann et al. 2016; Weindorf et al. 2012). A benefit of using morphometrics is in the exploration of within-horizon soil variations, which is often

overlooked in traditional soil pit descriptions. As an example, the first 27 or 30 cm of our soil profile was identified as Ap horizon, but the distribution of Ca concentration within this horizon was heterogeneous; the mean value ranged between 5908 mg kg^{-1} at 0–10 cm and 3753 mg kg^{-1} at 20−30 cm. Similarly, the mean pH also dropped from 6.3 at 0−10 cm to 5.9 at 20–30 cm. In case of Si, the upper 10 cm of Ap horizon was least variable (CV = 7 %) than the lower most 10 cm of it where the maximum variation was found (CV = 62 %). Grauer-Gray and Hartemink (2016) reported similar within-horizon variations in soil properties of a Mollisol profile wall.

Use of geostatistics, which is common in soil science (Burgess and Webster 1980; Goovaerts 1999), allowed us to evaluate autocorrelation and spatial variations of soil properties in the profile wall. Spatial prediction with block kriging represented our sample grid dimension. Grouping similar values of soil properties into more homogeneous classes is a key to clustering and it has been used in soil classification studies (e.g., Fajardo et al. 2015; McBratney and Gruijter 1992; Powell et al. 1992; Webster 1973).

12.4.2   Variation in Soil Profile Wall

Soil properties were variable in the profile wall and displayed a well spatial structure. Top 30 cm of the profile showed higher variation compared to lower horizons. All elements and θ displayed short-range variations compared to pH and red color which had a maximum range. All properties except Si had a strong spatial dependence. The level of Al and Si was lower in the surface and higher at 20 to 60 cm, whereas the levels of Fe, Mn, Ca, pH, and θ gradually decreased. Grauer-Gray and Hartemink (2016) found a lower Al in the surface soil horizons where the levels of Ca and soil pH were higher. The nature of Al and Si, which are related to clay minerals and their distribution in the profile, indicated that these soils have lost some clay from the surface horizons, which is illuviated below 40 cm. A second explanation is that the subsoils are enriched with aluminosilicate minerals through mineral weathering. The higher levels of Mn, Fe, Ca, and pH in the surface and their reduction with depth might be due to fertilizer application, irrigation, liming or leaching. Similar effect of liming and leaching on the depth function of pH and soil development has been reported from Denmark (Adhikari et al. 2014; Madsen and Munk 1987). Likewise, higher moisture in the surface could be linked to the irrigation. Although soil moisture is a dynamic property that is related to texture, structure, soil carbon, irrigation, and precipitation, its content as measured in the field is related to variation in soil texture and water-holding capacity (Mulla 1988; Reynolds 1970).

12.4.3 Identifying Horizon Boundaries

The *k*-means clustering identified three soil horizons in the profile. The boundary between cluster two (horizon Ap) and three (horizon Bw1) was determined by the levels of Si, Al, and Ca. Horizon Ap had the lowest levels of Al, and Si, but the highest level of Fe, Mn, and Ca. Horizon Bw1 was associated with the highest concentration of Al and Si. Horizon Bw2 had minimum Fe, Mn, and Ca. These findings suggest that aluminosilicate minerals, which are mostly related to clay content, were leached from Ap and illuviated in lower horizons, mostly in Bw1 or in situ formation of such minerals. The clustering technique was able to capture the influence of agricultural activities such as fertilization, irrigation, and liming that has increased the levels of Fe, Ca, and Mn on the surface soils for horizon boundary designation.

12.5 Conclusions

This study demonstrated the usefulness of digital soil morphometrics for mapping a profile wall with emphasis on the soil horizon boundary identification. The methodology presented is a way of identifying and locating soil horizon boundaries that would complement our pedological understanding. Based on the study, the following can be concluded:

- Fe, Mn, Ca, pH, and soil moisture decreased with soil depth, while red color value increased. Al and Si increased at a depth between 30 and 60 cm.
- Clusters of the kriged values of soil properties were able to locate three most probable soil horizons in the soil profile.
- The pXRF and soil color can be useful tools for soil horizon delineation.

References

Adhikari K, Kheir RB, Greve MB, Bøcher PK, Malone BP, Minasny B, McBratney AB, Greve MH (2013) High-resolution 3-D mapping of soil texture in Denmark. Soil Sci Soc Am J 77:860–876

Adhikari K, Kheir RB, Greve MB, Greve MH, Malone BP, Minasny B, McBratney AB (2014) Mapping soil pH and bulk density at multiple soil depths in Denmark. In: Arrouays D, McKenzie NJ, Hempel J, de Forges AR, McBratney AB (eds) GlobalSoilMap: basis of the global spatial soil information system. CRC Press/Balkema, Leiden, p 155

Beaudette DE, Roudier P, O'Geen AT (2013) Algorithms for quantitative pedology: a toolkit for soil scientists. Comput Geosci 52:258–268

Bockheim J, Gennadiyev A, Hammer R, Tandarich J (2005) Historical development of key concepts in pedology. Geoderma 124(1):23–36

Brady NC, Weil RR (1996) The nature and properties of soils. Prentice-Hall Inc.

Bridges EM (1993) Soil horizon designations; past use and future prospects. CATENA 20(4):363–373

Burgess TM, Webster R (1980) Optimal interpolation and isarithmic mapping of soil properties. 1. The semi-variogram and punctual kriging. J Soil Sci 31(2):315–331

Butler BE (1980) Soil classification for soil survey. Clarendon Press, Oxford

Cambardella CA, Moorman TB, Novak JM, Parkin TB, Karlen DL, Turco RF, Konopka AE (1994) Field-scale variability of soil properties in central Iowa soils. Soil Sci Soc Am J 58 (5):1501–1511

Chaplot V, Walter C, Curmi P, Hollier-Larousse A (2001) Mapping field-scale hydromorphic horizons using radio-MT electrical resistivity. Geoderma 102(1):61–74

Doolittle JA, Collins ME (1995) Use of soil information to determine application of ground penetrating radar. J Appl Geophys 33(1):101–108

Fajardo M, McBratney A, Whelan B (2015) Fuzzy clustering of Vis–NIR spectra for the objective recognition of soil morphological horizons in soil profiles. Geoderma (In press)

FitzPatrick EA (1988) Soil horizon designation and classification. International Soil Reference and Information Centre, ISRIC, Wageningen

Goovaerts P (1999) Geostatistics in soil science: state-of-the-art and perspectives. Geoderma 89(1–2):1–45

Grauer-Gray JR, Hartemink AE (2016) Variation of soil properties in a Mollisol profile wall. In: Hartemink AE, Minasny B (eds) Digital soil morphometrics. Springer, Dordrecht

Hartemink AE, Minasny B (2014) Towards digital soil morphometrics. Geoderma 230–231:305–317

Kellogg CE (1974) Soil genesis, classification, and cartography: 1924–1974. Geoderma 12 (4):347–362

MacQueen J (1967) Some methods for classification and analysis of multivariate observations. In: Proceedings of the fifth Berkeley symposium on mathematical statistics and probability. Oakland, CA, USA, pp 281–297

Madsen HB, Munk I (1987) The influence of texture, soil depth and geology on pH in farmland soils: a case study from southern Denmark. Acta Agriculturae Scandinavica 37(4):407–418

McBratney A, Gruijter JD (1992) A continuum approach to soil classification by modified fuzzy k-means with extragrades. J Soil Sci 43(1):159–175

Minasny B, McBratney AB, Whelan BM (2005) VESPER version 1.62. Australian Centre for Precision Agriculture, McMillan Building A05, The University of Sydney. NSW

Minasny B, Stockmann U, Hartemink AE, McBratney A (2016) Measuring & modelling soil depth functions. In: Hartemink AE, Minasny B (eds) Digital soil morphometrics. Springer, Dordrecht

Mulla D (1988) Estimating spatial patterns in water content, matric suction, and hydraulic conductivity. Soil Sci Soc Am J 52(6):1547–1553

Powell B, McBratney AB, MacLeod DA (1992) Fuzzy classification of soil profiles and horizons from the Lockyer Valley, Queensland. Australia. Geoderma 52(1–2):173–197

Reynolds S (1970) The gravimetric method of soil moisture determination part III an examination of factors influencing soil moisture variability. J Hydrol 11(3):288–300

Rooney D, Lowery B (2000) A profile cone penetrometer for mapping soil horizons. Soil Sci Soc Am J 64(6):2136–2139

SAS Institute Inc. (2013) Using JMP 11. Cary, NC, SAS Institute Inc.

Steffens M, Buddenbaum H (2013) Laboratory imaging spectroscopy of a stagnic Luvisol profile—high resolution soil characterisation, classification and mapping of elemental concentrations. Geoderma 195–196:122–132

Stockmann U, Jun Jang H, Minasny B, McBratney AB (2016) The effect of soil moisture and texture on Fe concentration using portable X-ray fluorescence spectrometers. In: Hartemink AE, Minasny B (eds) Digital soil morphometrics. Springer, Dordrecht

Tabbagh A, Dabas M, Hesse A, Panissod C (2000) Soil resistivity: a non-invasive tool to map soil structure horizonation. Geoderma 97(3):393–404

Triantafilis J, Ward W, Odeh I, McBratney A (2001) Creation and interpolation of continuous soil layer classes in the lower Namoi valley. Soil Sci Soc Am J 65(2):403–413

USDA (1999) Soil taxonomy: a basic system of soil classification for making and interpreting soil surveys, 436. US Department of Agriculture, Soil Conservation Service

Webster R (1973) Automatic soil-boundary location from transect data. J Int Assoc Math Geol 5 (1):27–37

Weindorf DC, Zhu Y, Haggard B, Lofton J, Chakraborty S, Bakr N, Zhang W, Weindorf WC, Legoria M (2012) Enhanced pedon horizonation using portable X-ray fluorescence spectrometry. Soil Sci Soc Am J 76(2):522–531